Numerical Modeling of a Deoxyribonucleic Acid Microassay: Carbon Nanotube Thin Film Transistor Sensor

Akin Akturk[†], Neil Goldsman[†], Herman Pandana[†], Romel Gomez[†]
[†] Department of Electrical and Computer Engineering
University of Maryland, College Park, MD, USA

Javed Khan[‡]
[‡] Pediatric Oncology Institute, National Cancer Institute
National Institutes of Health, Gaithersburg, MD, USA

***Abstract*—We develop numerical modeling techniques to investigate the electrical performance of a deoxyribonucleic acid (DNA) microsensor that uses a carbon nanotube thin film transistor (CN-TFT), and obtain agreement with experiment. This DNA microassay is developed to electrically sense low concentrations (pico to nano Molars) of specific DNA strands without requiring the use of labels such as fluorescent markers.**

Keywords-DNA microassay, carbon nanotube, thin film transistor, label-free microassay.

I. INTRODUCTION

Research on deoxyribonucleic acid (DNA) microassays, which are sensor modules for detecting specific DNA strands, [1,2] is ever-expanding, as health professionals and companies are demanding portable, multiple-use, easy-to-operate biosensors for quick-turn-around and low-cost DNA analyses. Label-free electrical detection of specific DNA strands offers such portability, low-cost and fast response, and hence DNA microassays based on this principle are being developed to obtain their sensitivity limits and feasibility.

The operation of these label-free electrical sensors relies on detecting the electronic charge on the phosphate backbone of the DNA. The phosphate group that is on each DNA strand ionizes as DNA dissolves in an electrolyte buffer solution. Therefore total amount of these phosphate groups and the associated electronic charges doubles at places where Watson-Crick hybridizations take place.

As DNA microassays, we use carbon nanotube thin film transistor (CN-TFT) sensors [1], as shown in Fig. 1. Such a sensor is comprised of a sensing plate, which is a mat of carbon nanotubes in the device channel, and a probe plate, which is composed of single-strand sense DNAs attached on top of the device gate. There is an electrolyte buffer between the gate oxide and the gate probe, and this buffer contains a tissue extract, which includes target DNAs, after lysis and possible DNA amplification, and salt for aiding DNA hybridizations. Further, the chemical hybridization reactions occurring at the probe plate between sense DNAs and their complementary target DNAs are translated into electrical signals in the sense plate, which is physically isolated from the probe plate and the electrolyte buffer by the gate oxide.

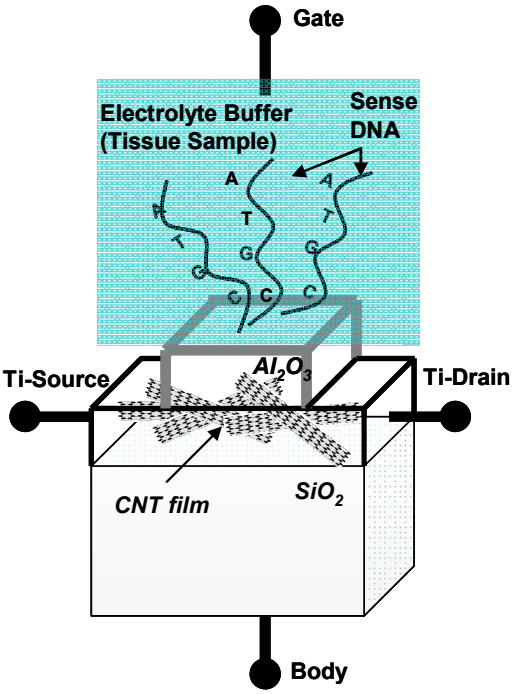

Figure 1. Simulated CN-TFT with titanium source-drain terminals, and a CN thin film in the channel. Sense DNAs are chemically attached to its gate oxide. Shaded region above the gate oxide is a tissue sample (electrolyte buffer). This sample includes the target DNAs, which are complementaries of the sense DNAs, we want to detect.

Target DNA hybridizations with sense probe DNAs give rise to threshold voltage shifts in CN-TFTs. These shifts, which are linearly proportional to the amount of hybridizations at the gate and inversely proportional to the total gate capacitance, then result in changes, namely horizontal shifts, in current-voltage curves of the CN-TFT, which has a mat of variety of tubes in the active device channel.

Here, our goal is to characterize the overall operation using a multi-pronged approach: First we examine how the tissue sample, which has target DNAs and sits on top of the CN-TFT

978-1-4244-1753-7/08/$25.00 ©2008 IEEE

gate oxide, reacts to the applied bias, and how much of the target DNA can be pushed against the sense DNA to achieve maximum output signal. Upon DNA hybridization the flatband voltage of the CN-TFT changes, thereby causing a shift in the current-voltage curves. Therefore in conjunction with experiments we then investigate device performance of CN-TFTs, and changes in output characteristics as a function of DNA hybridization.

II. Numerical Modeling

To investigate the performance of a CN-TFT-based DNA microassay, we develop a device simulator that is capable of obtaining electrical performance figures such as current-voltage curves of a field-effect-transistor (FET) incorporating individual CNs of varying diameters and chiralities, or wrapping angles. This requires determination of the governing differential device equations and the electrical CN parameters. First, to obtain the electrical CN parameters as a function of diameter, chirality and length, we develop models based on the first physical principles. This provides CN subband structure and mobility to be used in the device simulator. Then, at the device level, we determine the governing physics that resolves transport and quantization in the CN and the surrounding material in the longitudinal and transverse directions, as well as the barrier effects between the CN channel and its contact materials. This further requires the discretization of these equations into a suitable form for numerical analyses in two-dimensions. In addition to terminal current-voltage characteristics, the simulator provides a model for the change of the 'threshold voltage' with gate charge, and thus theoretically quantifies the sensitivity of the CN-FET to the amount of hybridization occurring on the gate terminal. In accordance with measurements, the electrical parameters that govern operation are calibrated until the theoretical and real performance match.

We extend the device simulating capability to determine electrical characteristics of an FET using an ensemble, or a mat, of CNs per transistor. In addition to the determination of electrical CN behavior, this requires characterization of the electrical CN mat, or thin film behavior. To obtain averaged electrical ensemble CN behavior, the electron transport or hopping between the tubes as well as transport in the tube needs to be resolved. Once the ensemble CN behavior is obtained, the results are incorporated into the CN-FET thin-film simulator. A model for the change of the 'threshold voltage' with gate charge for the ensemble CN-FET device is provided, and thus the sensitivity of the CN-FET to the amount of hybridization occurring on the gate terminal is theoretically quantified. The device simulator is developed in parallel with measurements in such a way that the experiments will validate the theoretical calculations.

Below to quantify the probe plate's impact on overall microassay operation, we first determine models that explain how the electrolyte or buffer solution, which include sense and target DNAs along with other ions and particulates, respond to an applied bias. Second, we show models that we use to investigate the CN-TFT's electrical performance at the sensing plate level.

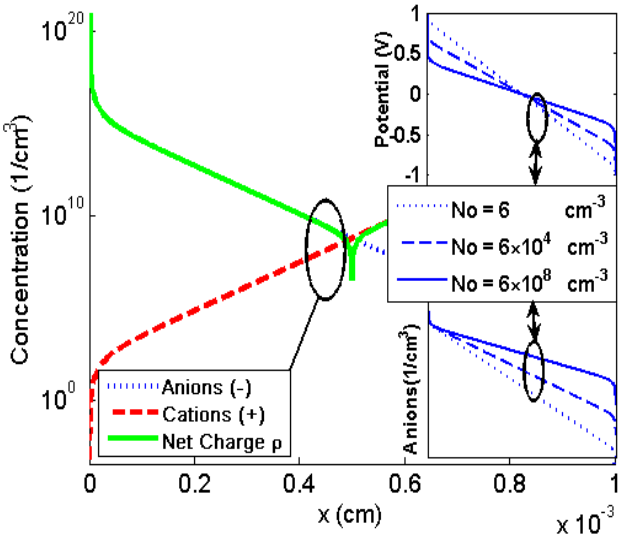

Figure 2. Anion (negatively charged), cation (positively charged) and net charge concentrations as a function of location under 2V applied bias and 6×10^8 cm^{-3} initial ion concentration. Insets show how the potential and anion concentration profiles change as a function of distance (0 to 10μm) for three different initial ion concentrations.

A. Modeling of Charge Distribution in an Electrolyte Buffer

Our DNA microassay is a hybrid of an ion-sensitive field effect transistor and a thin film transistor, as shown in Fig. 1. Here the ionic solution, which is a droplet from a tissue sample after lysis and possible DNA amplification, sits on top of the gate oxide. The single strand sense DNAs shown in Fig. 1 are physically attached to the gate oxide, and they hybridize only with their complementary (target) DNAs that we want to detect.

DNA hybridizations are affected by two main mechanisms: First is our ability to push target DNAs to the vicinity of sense DNAs by applying a voltage to a suspended gate electrode that touches the tissue sample from the top (Each DNA strand has a net positive charge). Second is setting the ambient conditions that are necessary for hybridization. These include high salt concentration, and ambient temperatures lower than DNA dissociation temperatures.

As a tissue sample is dropped onto the gate, there will be amphoteric reactions at the surface and a consequent electrolyte surface pile-up. Both of these can be controlled to some extent by changing the ionic composition or pH of the sample. The concentration profile of the rest of the solution can be changed by applying a voltage. In this case, ionic charge distribution can be modeled using the Poisson-Nernst equation [3] written below.

$$\nabla^2\phi = -\frac{qN_o}{\varepsilon}\left[\exp\left(-\phi/V_{\text{th}}\right) - \exp\left(+\phi/V_{\text{th}}\right)\right] \qquad (1)$$

Here N_o is the ion concentration everywhere at zero bias, ε ($=80\times\varepsilon_o$) is the dielectric constant of water, ϕ is the

electrostatic potential, q is the electronic charge and V_{th} is the thermal voltage.

Fig. 2 shows our calculated anion and cation concentrations under 2V bias for an initial ion concentration of 6×10^{8} cm^{-3}. The insets indicate that for a high initial concentration, most of the anions and cations can be pushed against positively and negatively biased plates, respectively. For low concentration values, a fraction of carriers can be piled up at the edges. Thus we may not be able to push all target DNAs near sense DNAs for hybridization and a subsequent detection.

In the electrolyte buffer, we have salt ions such as Na^{+}, Cl^{-} and P^{+} in addition to the ionized DNA strands. Therefore the ion concentration can be much larger than the DNA concentration. High salt concentration facilitates DNA hybridization. However, a high salt concentration also corresponds to a large diffusion capacitance that hinders CN-TFT operation (This capacitance is also called the Debye capacitance).

An approximate value for this diffusion capacitance can be calculated by taking the potential integral of both sides of (1), and relating the electric field to total charge. This gives the following relation between the total net charge Q and applied voltage V.

$$|Q| = (8\varepsilon N_o kT)^{1/2} \sinh\left(V / 2V_{th}\right) \qquad (2)$$

For low applied biases, the hyperbolic sinusoid can be approximated by its argument, and an analytical formula for the Debye capacitance can be written as follows.

$$C_{Debye} = \frac{(8\varepsilon N_o kT)^{1/2}}{2V_{th}} \qquad (3)$$

To calculate the total threshold voltage shift, gate oxide capacitance as well as the Debye capacitance need to be considered as the latter often limits the sensitivity. In the case of large applied biases, numerical solutions such as those shown in Fig. 2 can be employed to calculate a value for the Debye capacitance.

B. Performance Modeling of the DNA Microassay: CN-TFT Sensor

To obtain device performance of the CN-TFT, we self-consistently solve the coupled semiconductor (electron and hole current continuity) equations and the Poisson equation, respectively written below, including the barrier effects (due to differences in affinities and densities-of-states) between the source-drain metal (Ti) and the thin CN-film channel [4,5].

$$\frac{\partial n}{\partial t} = \nabla.\left(-n\mu_n \nabla\left(\phi + \phi^{n}_{Ti-CN}\right) + \mu_n V_{th} \nabla n\right) + G^{n} \qquad (4)$$

$$\frac{\partial p}{\partial t} = \nabla.\left(p\mu_p \nabla\left(\phi + \phi^{p}_{Ti-CN}\right) + \mu_p V_{th} \nabla p\right) + G^{p} \qquad (5)$$

$$\nabla^2 \phi = -\frac{q}{\varepsilon}\left(p - n + D\right) \qquad (6)$$

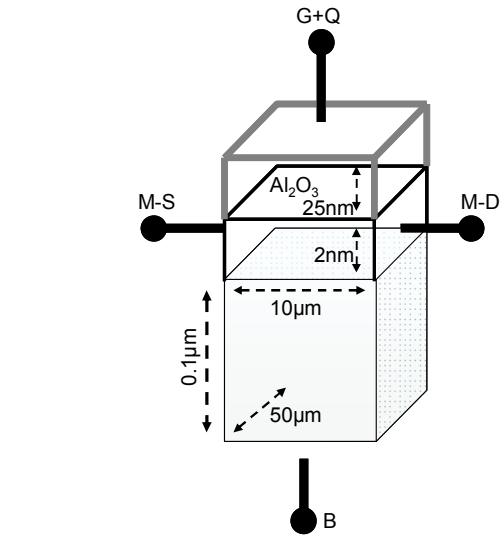

a)

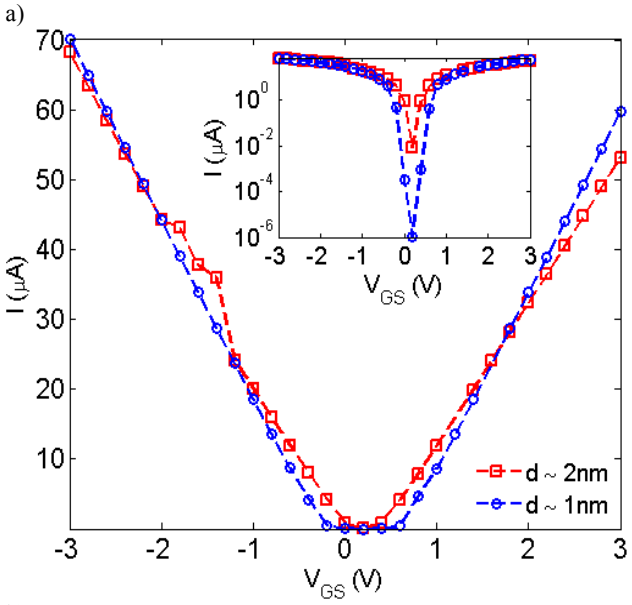

b)

Figure 3. a) Simulated CN-TFT sensor with a silver gate above an electrolyte buffer, titanium (with a work function of 4.3 eV) source-drain terminals, W/L = 50/10 (μm/μm) and t_{ox} = 25 nm. b) Calculated ambipolar current-voltage curves of a CN-TFT with CN mats composed of approximately 1 nm and 2nm diameter tubes,. Inset shows the same curves in a logarithmic scale.

Above, electron concentration is n; hole concentration is p; electrostatic potential is ϕ; carrier mobilities are μ_n and μ_p; net carrier generation-recombination rates are G^n and G^p; and electron and hole barrier effective potentials that arise due to the metal terminal and the CN channel are ϕ^{n}_{Ti-CN} and ϕ^{p}_{Ti-CN}, respectively. The other parameters in the preceding equations have their usual or aforementioned meanings.

Here, the barrier effective potentials account for the differences in electron affinities and densities of states on either side of the contact material and the CN thin film barrier. This

formalism for the barrier can resolve the thermionic emission current, which is the main transport mechanism for Schottky-type metal/semiconductor junctions with small barriers. As the source and drain contacts made out of titanium, and the channel is formed by carbon nanotubes, we expect the thermionic-type conduction to dominate over tunneling. For large barrier heights (after effects of mirror charges are subtracted from the barrier height), the latter may play a more important role than the former tunneling.

III. Comparison Of Calculated And Measured Results

Our fabricated CN-TFT sensors [1] are shown in Figs. 1 and 3a. To summarize, we have titanium source-drain terminals, an electrolyte above the sapphire gate oxide with a thickness of 25 nm, a suspended silver gate electrode, device width of 50 μm, and device length of 10 μm, as shown in Fig. 3a.

Our calculated results for the device in Fig. 3a obtained by solving coupled differential equations (4) to (6) are shown in Fig. 3b. We take the average diameter of the tubes forming the channel mat as 1 nm or 2 nm. Increasing this diameter from 1 nm to 3 nm slightly lowers current values at gate biases further away from the current minimum, and increases the leakage current around 1 V gate bias, as larger diameter tubes have lower bandgaps. Furthermore, we decrease the measured currents by approximately a constant 14 μA to remove leakage current due to metallic tubes in the CN-film (these metallic tubes are currently burnt ("zapped") using self-heating to diminish their contribution to the overall current). Here we have ambipolar conduction due to increased probability to overcome band barriers for electrons (holes) at high (low) gate biases due to use of titanium with a work function of 4.3 eV at the source and drain (we use 4.4 eV as the CN-film work function). Additionally, the mat itself being slightly p-type along with the work function of the gate metal and the charge due to DNA hybridizations causes the minimum of the current-voltage curves to shift to slightly positive gate-to-source biases.

Each DNA strand is positively charged due to the phosphate backbone of the DNA. As Watson-Crick DNA hybridizations occur between target DNAs in the tissue sample and sense DNAs attached to the gate oxide, the minimum of the current-voltage curve shifts. Emergence of additional charges associated with newly-binding or target DNA strands just above the gate surface change the threshold voltage, and shift the entire current-voltage curve shown in Fig. 3 to the right, towards higher gate biases. We then measure this shift, and correlate it with different amounts of DNAs that hybridize.

Figure 4 shows agreement between our measured [1] and calculated ambipolar current-voltage curves of a CN-TFT, similar to the one shown in Fig. 1. In our simulations, we take average CN diameter in the CN-film as 1 nm. The current minimum is measured at roughly 1 V gate-to-source bias. The maximum current value for the gate-to-source bias range is measured to be approximately 25 μA. For electrolytes with nano-molar DNA concentrations, the mean shift in threshold voltage is measured as approximately several tens of millivolts, while it is approaching hundred millivolts for micro-molar

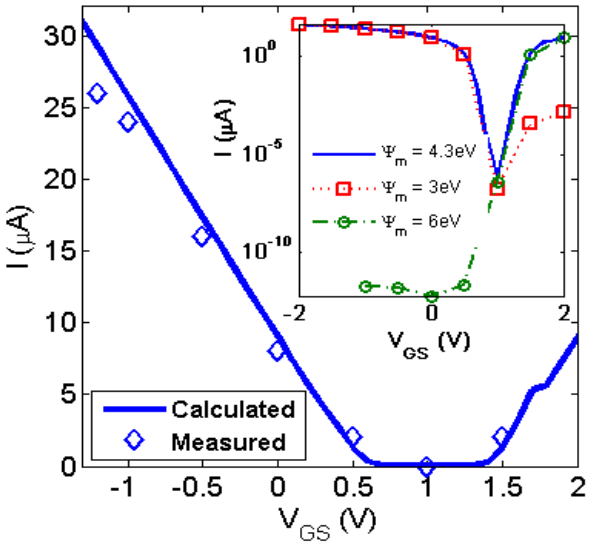

Figure 4. Calculated and measured [1] ambipolar current-voltage curves of the CN-TFT shown in Fig. 3a. Inset shows that use of different affinity materials at the source and drain will result in ambipolar (n- and p-type) or single-carrier conduction.

concentrations [1]. Further, Fig. 4 inset shows that using metals with different work functions at the source and drain, we may have bipolar or only n- or p-type conduction.

IV. Conclusion

In conclusion, we examine the performance of CN-TFT sensors that are used as DNA microassays. This is achieved at two levels: First, we investigate the response of an electrolyte buffer to an applied bias to quantify the percentage of target DNAs that would move to the close proximity of sense DNAs for probable hybridization. This also gives the diffusion capacitance associated with the electrolyte buffer. While high salt concentration helps Watson-Crick hybridizations, it also gives rise to high diffusion capacitance. Second, we analyze the operation of CN-TFT sensor, and obtain agreement between calculations and measurements.

References

[1] H. Pandana, K. H. Aschenbach, D. S. Lenski, M. S. Fuhrer, J. Khan, and R. D. Gomez, "A versatile biomolecular charge-based sensor using oxide-gated carbon nanotube transistor arrays", IEEE Sensors Journal, vol. 8(6), pp. 655-660, 2008.

[2] G. K. Geiss *et al.*, "Direct multiplexed measurement of gene expression with color-coded probe pairs", Nature Biotechnology, vol. 26(3), pp. 317-325, 2008.

[3] C. D. Fung, P. W. Cheung, and W. H. Ko, "A generalized theory of an electrolyte-insulator-semiconductor field-effect transistor", IEEE Trans. on Electron Devices, vol. 33(1), pp. 8-18, 1986.

[4] A. Akturk, N. Goldsman, G. Metze, "Coupled simulation of device performance and heating of vertically stacked three-dimensional integrated circuits", Proceedings of SISPAD, pp. 115–118, Sept. 2005.

[5] A. Akturk, N. Goldsman, G. Metze, "Self-consistent modeling of heating and mosfet performance in three-dimensional integrated circuits", IEEE Transactions on Electron Devices, vol. 52(11), pp. 2395-2403, 2005.